Non-Steady Astrophysical Spiral Jets driven by Magnetic Collapse and Pressure

Jun-ichi Sakai

Department of Applied Mathematics and Physics, Faculty of Engineering,
Toyama University, Toyama, 930 Japan

ABSTRACT

A simple theoretical model of non-steady, astrophysical, spiral, two sided jets is investigated by means of the ideal MHD equations with the adiabatic law for both cases; $\gamma=5/3$ (ion dominated plasma) and $\gamma=4/3$ (radiation dominated plasma). It is shown that the combined effects of the radial magnetic pinch (magnetic collapse) and anisotropic plasma pressure can explosively produce super-Alfvénic two sided jets with the spiral structure. The high energy particle acceleration during the explosive jet formation is also briefly discussed.

1. INTRODUCTION

The astrophysical jets with the narrow, elongated features are observed in a variety of astrophysical objects: long relativistic jets ($\geq 10^6$pc) from active galactic nuclei (Begelman Blandford and Rees 1984; Bridle and Perley 1984), a pair of precessing jets from SS433 (Margon 1984), bipolar outflow (≤ 1pc) from young stellar objects (Lada 1985, Shu, Adams and Lizano 1987) and spray in solar flares (Svestka 1976).

It seems that there exist the general physical mechanisms (Konigl 1986) which give rise to similar manifestations (highly collimation, two sided jets in most cases, origination in compact objects and assosiation with magnetic fields) of the jets in these widely different scales.

The role of magnetic fields in the astrophysical jets has been considered mainly for the confinement and stability of the jets (see Begelman, Blandford and Rees 1984; Koupelis and Van Horn 1988 reference therein). As briefly summarized by Koupelis and Van Horn (1988), the electromagnetic production mechanisms of the jets have been recently investigated. Among them, Blandford (1976) and Blandford and Payne (1982) considered a mechanism for extration of energy and angular momentum from the accretion disk and the central black hole. Lovelace, Wang and Sulkanen (1986) studied the steady structure of self-collimated, force free, electromagnetic jets. Shibata and Uchida (1985) have worked out the details of non-steady jet formation by solving numerically the ideal MHD equations. Koupelis and Van Horn (1988) presented a simple model for acceleration of jets in which both rotation and magnetic fields are

important. Haswell, Tajima and Sakai (1987) studied high energy particle acceleration by non-steady electromagnetic fields in the accretion disk. The magnetic acceleration mechanism of plasma jets in solar flares has been recently considered (Sakai 1988) in assosiation with the current loop coalescence model (Tajima, Brunel and Sakai 1982; Tajima et al. 1987) in solar flares.

The purpose of the present paper is to study the combined effects of magnetic collapse (plasma pinch effect) and plasma pressure which could produce non-steady, spiral, two sided astrophysical jets. The above combined acceleration mechanism which was applied to the solar jet case (Sakai 1988) has not been explored in detail, especially from a simplified theoretical model. We show that super-Alfvénic spiral, two sided jets (self-collimated by magnetic fields) can be explosively produced by the combined forces of $\mathbf{j}\times\mathbf{B}$, which causes the magnetic collapse and the pressure gradient which enchances the velocity of the jet.

We use the ideal MHD equations, which do not include characteristic scale length in their normalized equations. The results obtained from the ideal MHD equations can be applied to a variety of astrophysical jets on widely different scales. The important physical parameter which appears in the ideal MHD equations is the plasma βratio. As seen later, we find super-Alfvénic jets in relatively high β (≥ 1) plasmas with the temperature anisotropy.

We consider the intermediate region, $r_s \ll r \ll r_j$ where r_s is the Schwarzschild radius and r_s is $10^{33}(M/10^8 M_\odot)$cm, and r_j is the length of the jet. We do not address the details of the central engine which gives rise to energy supply as well as the global structure of production region of the jet, including the acceretion disk. We concentrate on the local jet production region ("funnel region") where plasma radial sporadic flows may be triggerd by the central massive object and from the non-accretion disk.

In section 2 we derive the basic equations describing the dynamics of the jets from the ideal MHD equations. In section 3 we present the numerical results which show that the spiral jets can be explosively accelerated within very rapid time scale. We find maximum jet velocities and acceleration times for both cases: ion dominated plasma ($\gamma = 5/3$) and radiation dominated plasma ($\gamma = 4/3$). In section 4 the non-steady electromagnetic fields produced during the jet formation are discussed in association with high energy particle acceleration. We also discuss the fast magnetosonic shock formation by the plasma rebound following the magnetic collapse.

In section 5 we summarize our results and discuss an application to the extragalactic jets.

2. CYLINDRICAL JET MODEL–BASIC EQUATIONS

We here derive basic equations describing the non-steady, spiral, two sided jets from the ideal MHD equations. The main driving forces leading to a mass outflow from a gravitationally bound system are the pressure gradient and the Lorentz force. The acceleration mechanism due to the pressure is called thermally-driven (or radiation pressure-driven) jet. While the acceleration mechanism due to the Lorentz force is called magnetically driven jet. In the previous studies the above two acceleration mechanism have been considered separately, except for the recent numerical simulations by Shibata and Uchida (1985). For the deep understanding of the jet production mechanisms, efforts of theoretical modeling are important, especially for the

understanding of the key physical parameters of the jet acceleration mechanisms.

The ideal MHD equations coupled with the adiabatic law of state are

$$\frac{\partial \rho}{\partial t}+\mathrm{div}(\rho \mathbf{v}) = 0, \tag{2.1}$$

$$\rho\left(\frac{\partial \mathbf{v}}{\partial t}+\mathbf{v}\cdot\nabla\mathbf{v}\right) = -\nabla p+\frac{1}{4\pi}\mathrm{rot}\mathbf{B}\times\mathbf{B}, \tag{2.2}$$

$$\frac{\partial \mathbf{B}}{\partial t} = \mathrm{rot}(\mathbf{v}\times\mathbf{B}), \tag{2,3}$$

$$\frac{\partial p}{\partial t}+\mathbf{v}\cdot\nabla p+\gamma p\,\mathrm{div}\,\mathbf{v}=0, \tag{2.4}$$

where we have neglected the gravitational force, which is a restraining force of the jets. In order to get mass outflow from the gravitationally bound system, the jet velocity should exceed the escape velocity determined from the gravitational force. The specific heat ratio γ is taken to be 5/3 or 4/3, depending on whether the plasma near the jet production region is supported primarily by ion dominated pressure or radiation pressure.

We employ here the cylindrical coordinate (r, ϕ, z) to make a model with cylindrical symmetric jets. Futhermore we assume the spiral jet flows associated with the spiral magnetic field structure as shown in Fig.1.

The simple velocity fields showing the spiral, two sided jets are given by

$$V_r = \frac{\dot{a}}{a},$$
$$V_\phi = \frac{\dot{c}_1}{c_1}, \tag{2.5}$$
$$V_z = \frac{\dot{b}}{b}z,$$

where the dot means the time derivative and time dependent scale factors $a(t)$, $b(t)$ and $c_1(t)$ are determined self-consistently later.

From the continuity equation (2.1) and (2.5), the density $\rho(t)$ can be exactly given as

$$\rho(t) = \frac{\rho_0}{a^2 b} \tag{2.6}$$

where ρ_0 is a constant. The density is uniform in space where the jet can be accelerated.

We assume the magnetic fields with the spiral structure as shown in Fig.1 as

$$B_r = b_1(t)r/\lambda,$$

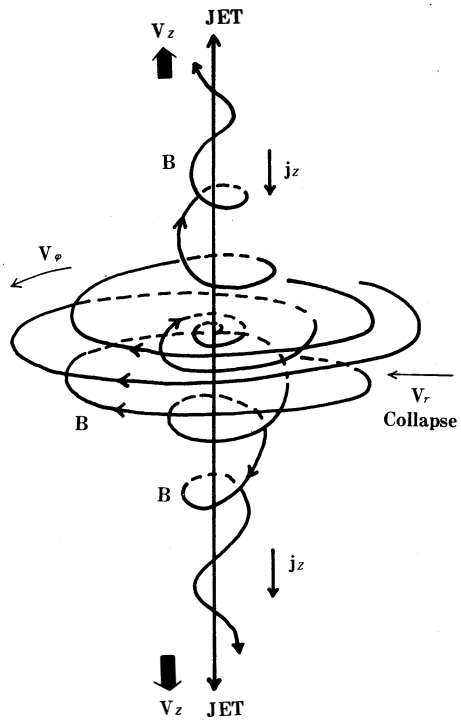

Figure 1. Shematic magnetic configuration (**B**) associated with the two sided spiral jets which can be driven by the magnetic collapse ($V_r<0$) and the pressure gradient. The plasma current (j_z) flows in the z-direction.

$$B_\phi = b_2(t)r/\lambda, \tag{2.7}$$

$$B_z = -2b_1(t)z/\lambda,$$

where $b_1(t)$ and $b_2(t)$ are determined, using the induction equation (2.3). λ is a characteristic scale lenght of variation of the magnetic fields. The above expression of the magnetic fields satisfies the equation, div $\mathbf{B} = 0$.

From equations (2.3) and (2.7), $b_1(t)$ and $b_2(t)$ are given by

$$b_1(t) = \frac{b_{10}}{a^2 b}, \tag{2.8}$$

$$b_2(t) = \frac{b_{20}}{a^2 b},$$

where b_{10} and b_{20} are constants. The plasma current is determined from the Maxwell equation; $\mathbf{J} = (c/4\pi)$ rot $\mathbf{B}$, which gives

$$j_z = \frac{cb_{20}}{2\pi\lambda a^2 b}, \tag{2.9}$$

$$j_\phi = j_r = 0.$$

Therefore the plasma current flows along the jet axis.

The plasma pressure p is assumed to be

$$p(r,z,t) = p_0(t) - \frac{p_{1r}(t)r^2 + p_{1z}(t)z^2}{2\lambda^2} \tag{2.10}$$

where $p_0(t)$, $p_{1r}(t)$ and $p_{1z}(t)$ are determined self-consistently later. The above expression means that the central region of the jet production can be heated by the central energy source which we do not address here. As seen in the next section, the jets can be explosively accelerated by the pressure anisotropy ($p_{1z} \gg p_{1r}$).

From the equations of motion (2.2), (2.5) − (2.8) and (2.10), we find the following equations for the scale factors, $a(t)$, $b(t)$, and $c_1(t)$;

$$\frac{d^2a}{dt^2} = \frac{a^3 b p_{1r}}{\rho_0 \lambda^2} - \frac{2V_A{}^2}{\lambda^2 ab} + a\left(\frac{\dot{c}_1}{c_1}\right)^2, \tag{2,11}$$

$$\frac{d^2b}{dt^2} = \frac{a^2 b^2 p_{1z}}{\lambda^2 \rho_0}, \tag{2.12}$$

$$\frac{d^2c_1}{dt^2} = \frac{2V_{A2}{}^2 c_1}{\lambda^2 a^2 b} + \frac{\dot{c}_1{}^2}{c_1} - 2\frac{\dot{a}\dot{c}_1}{a}, \tag{2.13}$$

where $v_A = b_{20}/(4\pi\rho_0)^{1/2}$, $v_{A2}{}^2 = v_A{}^2(b_{10}/b_{20})$. The time dependent pressure coefficients, $p_0(t)$, $p_{1r}(t)$ and $p_{1z}(t)$ are determined from equation (2.4) as

$$p_0(t) = \frac{P_{00}}{(a^2 b)^\gamma},$$

$$p_{1r}(t) = \frac{p_{10}}{a^{2(\gamma+1)} b^\gamma}, \tag{2.14}$$

$$p_{1z}(t) = \frac{p_{10}}{a^{2\gamma} b^{\gamma+2}},$$

Substituting the above equation (2.14) into equations (2.11) and (2.12), we obtain the basic equations ((2.13), (2.15),(2.16)) describing the spiral, two sided jets;

$$\frac{d^2a}{dt^2} = \frac{{c_s}^2}{\lambda^2 a^{2\gamma-1} b^{\gamma-1}} - \frac{2{V_A}^2}{\lambda^2 ab} + a\left(\frac{\dot{c}_1}{c_1}\right)^2, \tag{2.15}$$

$$\frac{d^2b}{dt^2} = \frac{{c_s}^2}{\lambda^2 a^{2\gamma-2} b^{\gamma}}, \tag{2.16}$$

where $c_s = (p_{10}/\rho_0)^{1/2}$

The main driving forces for the production of jet are the second term of the right-handed side in equation (2.15) which corresponds to the $j_z \times B_\phi$ force and the right-handed side in equation (2.16), which shows the pressure gradient, $\partial p/\partial z$. The former force can drive the plasma collapse ($a \to 0$) in the radial direction (we call this magnetic collapse; see Sakai and Ohsawa, 1987) and enhance the pressure p_{1z}. The combined effect of the magnetic collapse and the pressure gradient can strongly accelerate the tow sided, spiral jets.

3. EXPLOSIVE SPIRAL JET

We present the results of numerical calculation of the basic equations (2.15), (2.16) and (2.13), which can be written in the normalized form;

$$\frac{d^2a}{dt^2} = \frac{\beta}{a^{2\gamma-1} b^{\gamma-1}} - \frac{2}{ab} + a\left(\frac{\dot{c}_1}{c_1}\right)^2, \tag{3.1}$$

$$\frac{d^2b}{dt^2} = \frac{\beta}{a^{2\gamma-2} b^{\gamma}}, \tag{3.2}$$

$$\frac{d^2c_1}{dt^2} = \left(\frac{b_{10}}{b_{20}}\right)\frac{2c_1}{a^2 b} + \frac{\dot{c}_1^{\,2}}{c_1} - \frac{2\dot{a}\dot{c}_1}{a}, \tag{3.3}$$

where $\beta = {c_s}^2/{v_A}^2$ is the plasma β ratio, which is determined from the Alfvén velocity $v_A = b_{20}/(4\pi\rho_0)^{1/2}$ and the sound velocity $c_s = (p_{10}/\rho_0)^{1/2}$ The time is normalized by $\tau_A = \lambda/v_A$. As seen in equations (3.1) − (3.3), the physical parameters characterizing the jet flows are β and b_{20}/b_{10}. The characteristic scale lenght λ is included only through the normalized time $\tau_A = \lambda/V_A$ Therefore, the ideal MHD equations are scale-free and results obtained from the equations (3.1) − (3.3) may be applicable for a variety of different scale jet phenomena. The most important parameter is the β ratio.

3.1 Initial conditions

The basic equations (3.1) − (3.3) are solved as the initial value problem. The normalized velocities are $v_r/v_A\,(r/\lambda) = \dot{a}/a$, $v_\phi/v_A\,(r/\lambda) = \dot{c}_1/c_1$, and $v_z/v_A\,(z/\lambda) = \dot{b}/b$. The normarized density is $\rho/\rho_0 = 1/a^2 b$, and the normarized magnetic fields are $B_r/b_{10}{}^{(r/\lambda)} = 1/a^2 b$, $B_\phi/b_{20}{}^{(r/\lambda)} = 1/a^2 b$,$B_z/b_{10}{}^{(z/\lambda)} = -2/a^2 b$.

We show some results where $a(t=0) = 10$, $b(t=0) = 0.01$, $\dot{a}(t=0) = -(10-0.1)$, $\dot{b}(t=0) = 10^{-8}$, $\dot{c}_1(t=0) = 1$,$c_1(t=0) = 10^{-6}$ are taken. Therefore initial physical values we used are $v_r/v_A(r/\lambda) = -(1.0-0.01)$, $v_\phi/v_A(r/\lambda) = 10^{-6}$, $v_z/v_A(z/\lambda) = 10^{-6}$, $\rho/\rho_0 = 1$, $B_r/b_{10}(r/\lambda) = 1$, $B_\phi/b_{20}(r/\lambda) = 1$, $B_z/b_{10}(z/\lambda) = -2$. We take here $b_{10} = b_{20} = -1$.

The initial velocities of v_ϕ, v_z are much smaller than the Alfvén velocity at $r = z = \lambda$.

However, we used relatively large radial velocity, which means that the initial sporadic infall from the accretion disk plasma to the central massive objects may trigger the astrophysical jets. And if there exists some dynamical tidal interaction between stars near the central massive objects, there may occur the sporadic radial inflows.

We consider the initial plasma pressure distribution given by equation (2.10), which can be rewritten using equation (2.14) as

$$p(t=0) = \frac{p_{00}}{a^{2\gamma} b^{\gamma}} \left\{ 1 - \frac{p_{10}}{p_{00} a^2} \left(\frac{r^2}{2\lambda^2} \right) - \frac{p_{10}}{p_{00} b^2} \left(\frac{z^2}{2\lambda^2} \right) \right\}, \qquad (3.4)$$

If we use $a(t=0) = 10$, $b(t=0) = 0.01$, the ratio of the pressure amplitudes between the radial component $p_{10}/p_{00}a^2$ and z − component, $p_{10}/p_{00}b^2$ is 10^{-6}, which means that there exists strong pressure anisotropy ($p_{1r} \ll p_{1z}$). As the density is uniform in our model, the pressure anisotropy corresponds to the temperature anisotropy ($T_{1r} \ll T_{1z}$). This temperature anisotropy may be realized when we consider the heat source from the central engine ($r = z \simeq 0$) and heat conduction along the magnetic fields. Near the central engine where the magnetic field strength is weak, there is no temperature anisotropy because of the spherical infall to the massive object. However, far from the central energy source there are magnetic fields which play an important role for the heat conduction. Near the equatorial plane ($z \simeq 0$) the main magnetic field has poloidal component B_ϕ ($\gg B_r, B_z$) as seen in Fig.1.

The heat conduction across the poloidal magnetic field B_ϕ can be strongly reduced compared with the direction parallel to the magnetic field. Therefore the radiative cooling may become dominate in the r-direction. While the magnetic field lines are almost along the jet axis (z-direction) in the region far from the central. The heat conductivity along the magnetic field is so high that the temperature in the z-direction may be retained with the same one as the central source. We may expect from the above discussion that there appears the temperature anisotropy near the jet production region.

3.2 Spiral magnetic field structure

The magnetic field structure associated with the plasma jet is axial symmetry ($\partial/\partial\phi = 0$). The components of the axisymmetric magnetic field $\boldsymbol{B}$ which lie in the meridional planes can be expressed in terms of the magnetic stream function ψ ;

$$B_r = -\frac{1}{r}\cdot\frac{\partial\psi}{\partial z},$$
$$B_z = \frac{1}{r}\cdot\frac{\partial\psi}{\partial r}, \qquad (3.5)$$

The magnetic stream function ψ in the axisymmetric case can be written as

$$\psi(r,z,t) = rA_\phi, \qquad (3.6)$$

in which A_ϕ is ϕ-component of the magnetic vector potential $\mathbf{A}$ ($\mathbf{B} = \mathrm{rot}\,\mathbf{A}$). From Eqs. (3.5) and (2.7), we find the magnetic stream function ψ (r,z,t) as

$$\psi(r,z,t) = -\frac{b_{10}}{a^2 b} r^2 z, \qquad (3.7)$$

It is easy to show that the magnetic lines of force lie on the magnetic surface $\psi(r,z,t) =$ con-

stant, because the equation of the magnetic lines of force in the meridional lanes ($dr/B_r = dz/B_z$) gives

$$d\psi = \frac{\partial \psi}{\partial r} dr + \frac{\partial \psi}{\partial z} dz = 0, \tag{3.8}$$

It is also easy to show that $\psi(r,z,t)$ is conserved, i.e.

$$\frac{d\psi}{dt} = \frac{\partial \psi}{\partial t} + \mathbf{v} \cdot \nabla \psi = 0, \tag{3.9}$$

by means of Eqs. (2.5) and (3.7). The conservation of ψ means that the axisymmetric magnetic surfaces ψ in an ideal conducting plasma move along the material. Therefore the global structure of the magnetic field topology can change in a self-similar form as shown in Fig.1 during the formation of the jet.

3.3 Acceleration time and maximum jet velocity

We show the results of the case, $\beta = 1$, $\gamma = 4/3$. Fig.2 shows the time history of the radial velocity v_r normalized by $(v_A r/\lambda)$, with the initial value $\dot{a}/a = -0.01$. The magnetic force can induce strong plasma collapse ($v_r < 0$) by the plasma pinch effect (magnetic collapse). During the magnetic collapse the explosive two sided, spiral jets can be generated as seen in Fig.3. On the same time the plasma rotational motion can also be triggered as seen in Fig.4.

The acceleration time getting to the maximum jet velocity is quite short and $0.04\ \tau_A$ for the case of Fig.3. The most important parameter controlling the maximum jet velocity is the plasma β ratio, rather than the initial radial velocity. Table 1 shows the summary of the results for various β ratio, $\gamma = 5/3$ and $4/3$. As seen in the table, the results for $\gamma = 5/3$ and $4/3$ are almost same. When β is small (for example, $\beta = 10^{-4}$), the maximum jet velocity is less than the Alfvén velocity at $z = \lambda$. However, the β increases, the maximum jet velocity becomes super-Alfvénic within very short time scale. The maximum velocity with high β (≥ 1) is almost same for the case of $\beta = 1$.

The density and the magnetic field components are proportional to $(a^2 b)^{-1}$, which time history is Fig.5.

Table 1. Maximum jet velocities and acceleration times for various plasma β ratio.

β \ γ	5/3		4/3	
	$V_{Z,Max}(V_A \frac{Z}{\lambda})$	Acceleration Time	$V_{Z,Max}(V_A \frac{Z}{\lambda})$	Acceleration Time
10^{-4}	0.707	0.97 (τ_A)	0.65	1.03(τ_A)
10^{-3}	1.77	0.39 (τ_A)	1.81	0.39(τ_A)
10^{-2}	5.64	0.12 (τ_A)	5.83	0.12(τ_A)
10^{-1}	18.75	0.033(τ_A)	19.4	0.04(τ_A)
1	56.0	0.015(τ_A)	58.0	0.02(τ_A)
10	56.25($C_S \frac{Z}{\lambda}$)	0.011(τ_A)	58.3 ($C_S \frac{Z}{\lambda}$)	0.01(τ_A)
10^2	56.25($C_S \frac{Z}{\lambda}$)	0.011(τ_A)	58.2 ($C_S \frac{Z}{\lambda}$)	0.01(τ_A)

As seen in Fig.2 there appears strong rebound flow after the magnetic collapse. Such strong rebound flow becomes super-Alfvénic when the β is small and can generate the fast magnetosonic shock waves.

When the temperature anisotropy is weak ($a \simeq b$ at $t = 0$), the jet speed becomes sub-Alfvénic and the acceleration time becomes long.

4. STRONG ELECTRIC FIELD AND SHOCK FORMATION DURING THE JET PRODUCTION

We here show the results of strong electric fieid produced during the jet formation. The electric field induced from time varying magnetic field during the jet formation may play an important role for high energy particle acceleration (Haswell, Tajima and Sakai 1987). The induced electric field **E** can be derived from the frozen condition $\mathbf{E} = -\mathbf{V}\times\mathbf{B}/c$, where **V** and **B** are given by equations (2.5) and (2.7). The components of the induced electric fields are given by

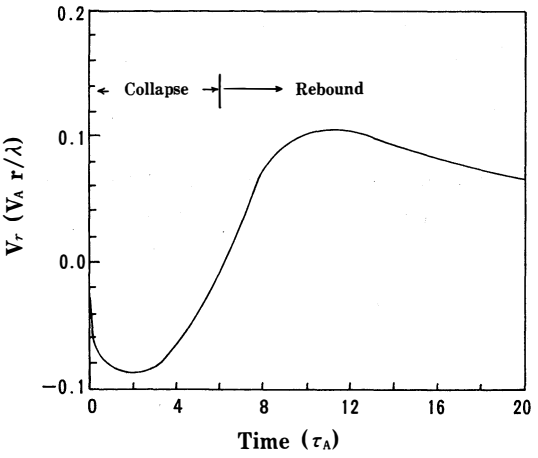

Figure 2. Time history of plasma radial velocity when $\beta = 1$, and $\gamma = 4/3$. The Lorentz force drives magnetic collapse, which enhances the rebound flow leading to the formation of fast magnetosonic shock waves.

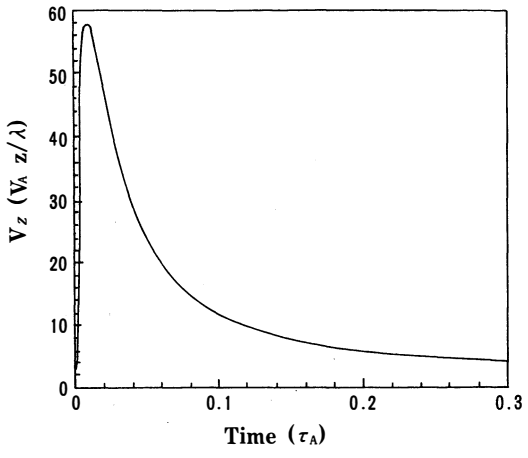

Figure 3. Time history of the jet velocity with $\beta = 1$ and $\gamma = 4/3$. The maximum velocity ($= 56.0\ v_A(z/\lambda)$) occurs at $t = 0.015\tau_A$.

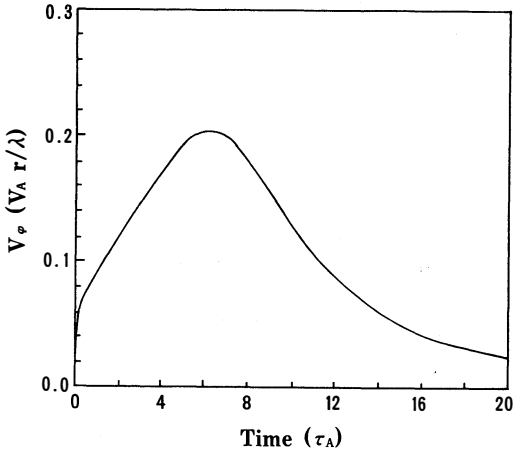

Figure 4. Time history of the velocity, v_ϕ with $\beta = 1$ and $\gamma = 4/3$.

$$E_r/E_0(rz/\lambda^2) = \left(2\frac{\dot{c}_1}{c_1}+\frac{b_{20}}{b_{10}}\cdot\frac{\dot{b}}{b}\right)/a^2b, \tag{4.1}$$

$$E_\phi/E_0(rz/\lambda^2) = -\left(\frac{\dot{b}}{b}+2\frac{\dot{a}}{a}\right)/a^2b, \tag{4.2}$$

$$E_z/E_0(r^2/\lambda^2) = \left(\frac{\dot{c}_1}{c_1}-\frac{b_{20}}{b_{10}}\cdot\frac{\dot{a}}{a}\right)/a^2b, \tag{4.3}$$

where $E_0 = b_{10}v_A/c$.

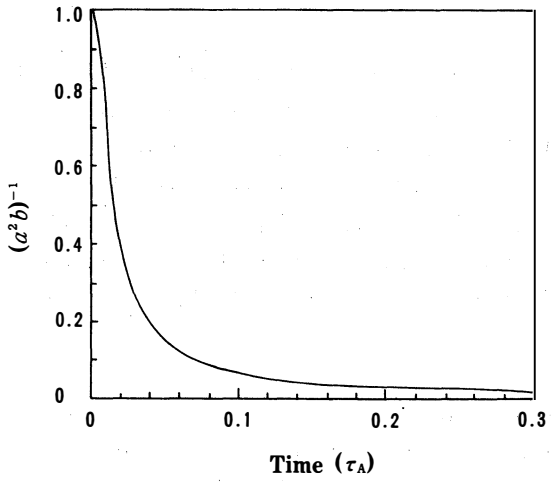

Figure 5. Time history of the density and the components of magnetic fields proportional to $(a^2b)^{-1}$ with $\beta = 1$, and $\gamma = 4/3$. The plasma current, j_z is also proportional to $(a^2b)^{-1}$.

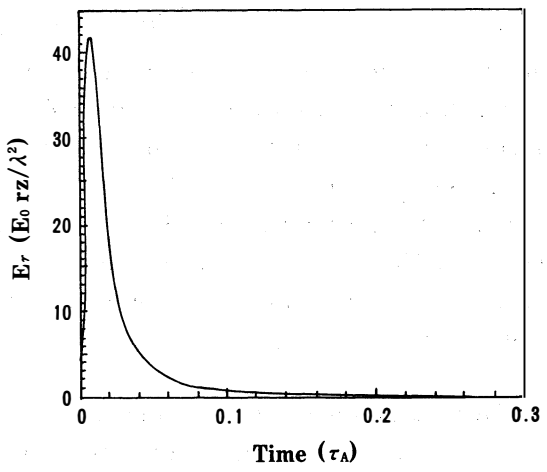

Figure 6 (a). Time history of electric field, E_r with $\beta = 1$ and $\gamma = 4/3$.

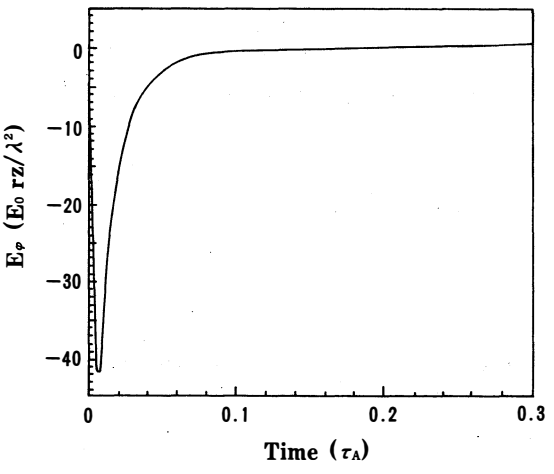

Figure 6 (b). Time history of electric field, E_ϕ with $\beta = 1$ and $\gamma = 4/3$.

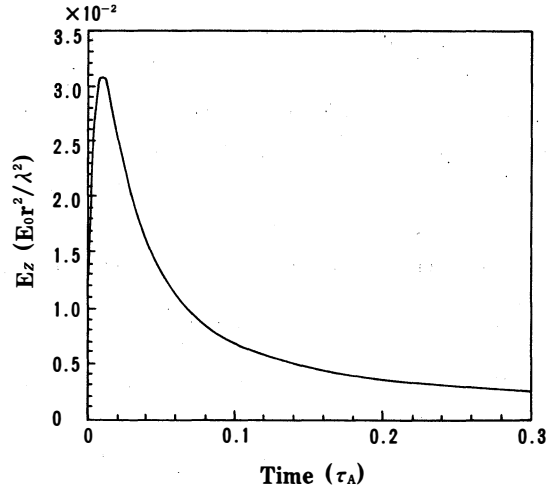

Figure 6 (c). Time history of electric field, E_z with $\beta = 1$ and $\gamma = 4/3$.

The time history of the above electric fields is shown in Fig.6 (a) – (c), when $b_{10} = b_{20} = -1$. During the explosive jet formation, strong electric fields can be generated. Near the peak of the electric fields these maximum amplitude can be retained during $10^{-2}\tau_A$, which time scale may be long many order of magnitude compared with the typical ion cyclotron period. Therefore if the typical high energy particle acceleration time is very short compared with $10^{-2}\tau_A$, the particle acceleration can be treated under the assumption of steady electromagnetic fields given by equations (2.7) and (4.1) – (4.3).

The equation of a test proton in its normalized form is

$$\frac{d\mathbf{P}}{dt} = \left(\frac{v_A}{c}\mathbf{E} + \frac{1}{\Gamma}\mathbf{P}\times\mathbf{B}\right), \tag{4.4}$$

where $\mathbf{P}$ is normalized by $m_i c$, time it is normalized by $\lambda/v_A = \omega_{ci}^{-1}$, $\mathbf{E}$ is normalized by E_0 and $\Gamma = (1+p^2)^{1/2}$. The particle with small $\mathbf{P}$ can be accelerated by the electric field of the first term of the right-handed side of equation (4.4). If $|(v_A/c)\mathbf{E}|$ is of order of unity, the particle can be easily accelerated to relativistic energy within very short time compared with $10^{-2}\tau_A$. The magnitude of the normalized electric fields, E_r and E_ϕ is about 40 as seen in Figs.6 (a) and 6 (b). Therefore $|(v_A/c)\mathbf{E}|$ can be of order of unity, even if v_A/c is 1/40. The details about the particle acceleration will be investigated by numerical calculations of the test particle (Sakai 1989).

4.1 Fast magnetosonic shock formation by plasma rebound

As seen in Fig.2 the plasma rebound following the strong plasma collapse may generate super-Alfvénic flow, which in turn can produce fast magnetosonic shock waves. The fast magnetosonic shock formation can occur when the local plasma flow velocity exceeds the local magnetosonic wave velocity; $v_r > (v_A^2 + c_s^2)^{1/2}$. This condition can be written as

$$\dot{ba} > 1 + \left(\frac{b_{10}}{b_{20}}\right)^2 + 4\left(\frac{b_{10}}{b_{20}}\right)^2\left(\frac{z}{r}\right)^2 + \frac{\beta}{a^{2\gamma-4}b^{\gamma-1}}\left\{\frac{p_{00}}{p_0}\left(\frac{r}{\lambda}\right)^2 - \frac{1}{2}\left(\frac{1}{a^4} + \frac{1}{b^2}\left(\frac{z}{r}\right)^2\right)\right\}, \tag{4.5}$$

For the low β case (where we neglect the last term of the right-handed side of equation (4.5)), the above condition becomes

$$\left[\dot{ba}^2 - \left\{1 + \left(\frac{b_{10}}{b_{20}}\right)^2\right\}\right]\left(\frac{r}{\lambda}\right)^2 > 4\left(\frac{b_{10}}{b_{20}}\right)^2\left(\frac{z}{\lambda}\right)^2, \tag{4.6}$$

If the parenthesis of the left-handed side in equation (4.6) is positive,

$$\sqrt{\dot{ba}} > \left\{1 + \left(\frac{b_{10}}{b_{20}}\right)^2\right\}^{1/2}, \tag{4.7}$$

the fast magnetosonic shock waves can be generated in the region where the following condition is satisfied;

$$\frac{r}{z} > 2\left|\frac{b_{10}}{b_{20}}\right| \cdot \left[\dot{ba}^2 - \left\{1 + \frac{b_{10}}{b_{20}}\right)^2\right\}\right]^{-1/2}, \tag{4.8}$$

where $|b_{10}/b_{20}|$ means the absolute value of b_{10}/b_{20}. The above condition, Eq. (4.7) can be satisfied in some cases. Figure 7 shows an example, where $b_{10} = b_{20} = -1$ and $\beta = 0.01$ are taken. We can find that the condition for shock formation. Eq. (4.7) can be satisfied in Fig.7.

The fast magnetosonic shock waves play an important role for plasma heating and high energy particle production (see review by Sakai and Ohsawa 1987).

5. SUMMARY AND DISCUSSION

We have shown that the spiral, two sided jets can be explosively generated by the combined two forces of magnetic Lorentz force and plasma pressure gradient. The important physical parameters characterizing the super-Alfvénic jet are the plasma β ratio and temperature anisotropy. The acceleration time to the maximum jet velocity is quite rapid of order of $0.01\tau_A$. We briefly discussed high energy particle acceleration by strong electric fields driven during the jet formation as well as by the fast magnetosonic shock waves produced by the plasma rebound following the magnetic collapse.

The MHD equations are scale-free equations so that the results obtained here can be applicable to a variety of astrophysical jet phenomena. Among them we consider an application to the extragalactic jet. For the extragalactic jet the central region of the jet formation can not be observed. If we take the scaie λ as $\lambda \sim 10^{14-15}$cm which is larger than the Schwartzshield radius $r_s = 10^{13}$ (M/8M⊙) cm for the central massive black hole and the Alfvén velocity $v_A \sim 10^{9-10}$cm/s (Begelman et al. 1984), the normalized time scale $\tau_A = \lambda / v_A = 10^{4-6}$sec. Therefore the acceleration time should be 10^{2-4}sec. From a theoretical argument (Begelman et al. 1984) the central region near the active galactic nucleus may be filled with the electron-positron plasma with the temperature $T \sim m_e c^2$. For the plasma with $\beta \sim 1$ we have $v_A \sim c_s = (m_e/m_i)^{1/2} c = 7 \times 10^8$cm/s. Therefore the maximum jet velocity may become relativistic velocity, $50 v_A \sim c$, as seen in Fig.3. In the previous discussion we have neglected the gravitational effect. The characteristic time scale T_k for the Keplerian motion around the central massive black hole is given by $T_k = 2\pi/\omega_k$, where $\omega_k = (GM/r^3)^{1/2}$. If we take $M = 10^8 M_\odot$, $r = 10^{14}$cm, T_k is 6×10^4 sec. If the acceleration time for the jet formation is less than T_k, we may neglect the Keplerian motion for the jet formation.

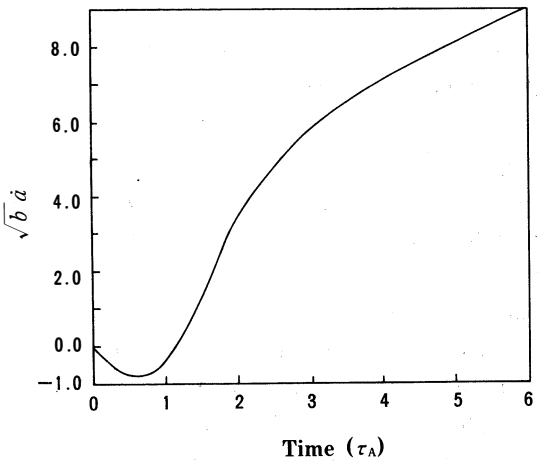

Figure 7. Condition for generation of the fast magnetosonic shock waves; after $\sqrt{b\dot{a}} > \sqrt{2}$ is satisfied when $b_{10} = b_{20} = -1$ and $\beta = 0.01$, the shock waves can be produced.

If the acceleration time becomes long, we need to take into account other physical process such as radiative cooling effect (Sakai 1989).

Because of non-relativistic MHD equations, the region of interest is assumed to be far from the Schwarzschild radius. However, the obtained solutions may approximate the solutions near the Schwarzschild radius. We assumed that initially $v_r < 0$. While, if we assume that initially rotational velocity occurs without mass inflow, we found that the rotational mass motion can

drive mass inflow and produce the similar plasma jets.

The obtained self-similar solutions which can exactly satisfy the MHD equations may represent local behaviour of the jet dynamics, because we don't solve exactly the MHD equations as initial-boundary value problem. However, the simple MHD jet solutions proposed here should give insight to the 3-D MHD simulation in the future.

ACKNOWLEDGEMENT

The author would like to thank Dr. Y. Ohsawa for helpful discussion. This paper was presented as an invited paper in joint Varenna-Abastumani Workshop on plasma Astroplysics, Varenna, Italy, August 24-Septenber 3, 1988. (ESA SP-285)

REFERENCES

Begelman, M.C., Blandford, R. D., and Rees, M.J. 1984, Rev. Mod. Phys., 56, 255.
Blandford, R.D. 1976, Mon. Not. R.. Astro. Soc., 176, 465.
Blandford, R.D., and Payne,D.G. 1982, Mon. Not. R. Astro. soc. 199, 883.
Bridle. A.H., and Perley, R. A 1984, Ann. Rev. Astro. Ap. 22, 319.
Haswell, C.A,Tajima, T., and Sakai, J-I. 1988, preprint.
Konigl, A. 1986, Ann. NY. Acad. Sci. 88.
Koupelis, T., and Van Horn, H. M. 1988, Ap.J. 324, 93.
Lada,C. J. 1985, Ann. Rev. Astro. Ap. 23, 267.
Lovelace, R.V.E., Wang,J.C.L., and Sulkanen, M.E. 1986, Ap. J. 315, 504.
Margon, B. 1984, Ann. Rev. Astro. Ap. 22, 507.
Sakai, J-I. 1989, Solar Phys. in press.
Sakai, J-I. 1989, in preparation.
Sakai, J-I., and Ohsawa,Y. 1987, Space Sci. Rev. 46, 113.
Shibata, K., and Uchida,Y. 1985, Pub. Astr. Soc. Japan. 37, 31.
Shu, F.H., Adams,F.C., and Lizano,S. 1987, Ann. Rev. Astro. Ap. 25, 25.
Svestka, Z. 1976, Solar Flares (Dordrecht: Reidel)
Tajima, T., Brunel,F., and Sakai,J-I. 1982, Ap. J. 245, L45.
Tajima, T., Sakai,J-I., Nakajima,H., Kosugi,T., Brunel,F., and Kundu,M.R. 1987, Ap. J. 321, 1031.

(Received October, 31 1988)